Surface Interactions between Boundary Layers of Poly(ethylene oxide)-Liposome Complexes

Surface interactions between boundary layers of poly(ethylene oxide)-liposome complexes: lubrication, bridging and selective ligation♦

S.A. Angayarkanni, Nir Kampf and Jacob Klein*

Department of Materials and Interfaces, Weizmann Institute of Science, Rehovot 76100, Israel

*corresponding author, e-mail: Jacob.Klein@weizmann.ac.il

♦ We dedicate this paper to the memory of Jacob Israelachvili, a great scientist and a path-breaking pioneer in the measurement and understanding of surface interactions

Abstract:

Poly(ethylene oxide), PEO, is widely exploited in biomedical applications, while phosphatidylcholine (PC) lipids (in the form of bilayers or liposomes) have been identified as very efficient boundary lubricants in aqueous media. Here we examine, using a surface force balance (SFB), the interactions between surface-adsorbed layers of PEO complexed with small unilamellar vesicles (SUVs, i.e. liposomes) or with bilayers of PC lipids, both well below and a little above their main gel-to-liquid phase transition temperatures T_M. The morphology of PEO layers (adsorbed onto mica), to which liposomes were added, was examined using atomic force microscopy (AFM) and cryo-scanning electron microscopy (cryo-SEM). Our results reveal that the PC lipids could attach to the PEO either as vesicles or as bilayers, depending on whether they were above or below T_M. Under water (no added salt), excellent lubrication, with friction coefficients down to $10^{-3} – 10^{-4}$, up to contact stresses of 6.5 MPa (comparable with those in the major joints) was observed between two surfaces bearing such PEO-PC complexes. At 0.1M KNO_3 salt concentrations (comparable with physiological salt levels) the friction between such surfaces was considerably higher, attributed to bridging by the polymer chains. Remarkably, such bridging could be suppressed, and the friction restored to its previous low value, if the KNO_3 was replaced by $NaNO_3$, due to the different PEO-mica ligation properties of Na^+ compared to K^+. Our results provide insight into the properties of PEO-PC complexes in potential applications, and to large interfacial effects that can result from seemingly innocuous replacement of K^+ by Na^+ ions.

Keywords: Lubrication, biolubrication, Poly(ethylene oxide), PEO, Poly(ethylene glycol), PEG, polymer bridging, phosphatidylcholine lipids, liposomes, hydration lubrication, selective ligation.

Introduction:

Liposomes are large-spherical vesicles consisting of phospholipids that form self-closed bilayer membranes.[1] They are biocompatible, with low toxicity[2] and are of much interests in applications related to drug delivery, gene delivery and vaccines.[3] Phosphatidylcholine (PC) lipids complexed with hyaluronan (HA) have been proposed to form strongly-lubricating boundary layers at biosurfaces such as articular cartilage.[4-6] Aqueous lubrication by surface attached phospholipids has been widely studied in recent years.[7-10] Depending on the type of PC used, efficient lubrication with friction coefficients down to 10^{-4} up to physiologically-high pressures (~100 atm)[9] has been observed. This was attributed to hydration lubrication, acting at the highly hydrated phosphocholine headgroups of the PC lipids exposed at the liposome surfaces.[11] Such hydration layers can sustain large compressions without being squeezed out from the gap between sliding surfaces.[12] At the same time, the hydration shells can relax rapidly, ensuring a fluid like response on shear, and this combination low shear stresses while sliding under high normal stresses results in very low friction coefficients μ (μ = (force to slide)/load), an effect termed hydration lubrication.[13] Several studies in recent years examined the lubrication by such PC vesicles on bare mica surfaces.[8,9] Gaisinskaya-Kipnis and Klein[14] investigated the lubrication of PC lipids complexed with a negatively-charged biomolecular bilayer (chitosan and alginate) adsorbed on a mica surface. We now extend this study to the case of a neutral water-soluble polymer, poly(ethylene oxide), PEO (also known as poly(ethylene glycol) or PEG) adsorbed on mica surfaces. PEO has some unique features: it is soluble in both water and organic solvents, and is widely used in stabilization of colloidal dispersions. It is also currently used in a wide variety of biomedical applications such as to improve the stability and biological performance of colloidal drug carriers,[15] including liposomic carriers, drug encapsulation,[16-19] pharmaceutical properties of therapeutic proteins,[20-24] and in antimicrobial/antifouling applications.[25-31] PEG-DSPE (distearylphosphatidylcholine) block copolymers are biocompatible and can be incorporated in lipid vesicles as stabilizers. PEG-based

hydrogels are also used in tissue engineering[32-34] and as scaffolds for cartilage repair,[35-39] while the surface of liposomes coated with poly(ethylene glycol) could be used for oral delivery of peptides[40] and vaccines.[41] In the present study, we use the surface force balance (SFB) to examine interactions between PEO layers adsorbed on mica and in particular how normal interactions and especially frictional interactions, are modified when PC liposomes are added in pure water and in aqueous salt solutions. Two PC lipids were used: dimyristoylphosphatidylcholine (DMPC, T_M = 24 °C) and distearoylphosphatidylcholine (DSPC, T_M = 55 °C), since it is known[9] that the lubrication properties of PC lipids can vary significantly with the main liquid-phase to gel-phase transition temperature T_M. For the case of the DSPC liposomes we investigated the behavior both under water and at physiological-level salt concentrations.

Materials and Methods

Materials:

Hydrogen peroxide (H_2O_2, 30%), concentrated sulfuric acid (H_2SO_4, 98%) and nitric acid (HNO_3, 70%) were supplied by Fisher Scientific, UK and used as received. Ethanol (absolute, HPLC grade, J.T Baker) was dispensed through a 0.45 μm pore-sized polyethersulphone membrane filter from a pressure rinser (Pall Corporation, USA). Water was purified by Barnstead NANOpure Diamond™ system, having total organic carbon (TOC) < 1 ppb and resistivity of 18.2 Ωcm at 25 °C (sometimes designated conductivity water). Ruby Muscovite mica (ASTM V-2, special grade) was purchased from S&J Trading Inc., New York. EPON® resin 1004F (Shell) was used to glue the mica pieces onto plano-cylindrical quartz lenses. Silver (99.9999%) was purchased from Sigma-Aldrich. Prior to every experiment, the glassware was cleaned in piranha solution (70% H_2SO_4, 30% H_2O_2. Care must be used as such solutions are extremely corrosive and can be dangerous if not handled correctly) and sonicated in pure water and ethanol for 10 min. Stainless steel tools were passivated in 50% aqueous HNO_3 followed by sonication in pure water and ethanol for 10 min each.

All preparations were carried out in a laminar hood to avoid particulate contamination. Potassium nitrate (KNO_3, 99.99% Suprapur®) was purchased from Mercury. Poly (ethylene oxide) of molecular weight 110 kDa and 26 kDa was purchased from PSS polymer standard services. The chemicals above were used as received without further purification. DSPC (18:0) and DMPC (14:0) were purchased from Lipoid (Ludwigshafen, Germany).

Liposome Preparation:

As-received lipids were dispersed in water. In order to obtain dispersed multilamellar vesicles (MLV), the lipids solution was sonicated for 5 minutes at 65 °C (DSPC) and at 35 °C (DMPC) , above the phase transition temperature of each lipid. Then the MLVs were progressively downsized using an extruder (Northern lipid Inc., Burnaby, BC, Canada) through polycarbonate filters having pore size of 0.4 μm (5 times) , 0.1 μm (8 times) and 0.05 μm (10 times). The size of the prepared liposomes were determined using dynamic light scattering (DLS). For the salt experiments the procedure was identical save that 0.1M KNO_3 solution was used in place of water.

Layer-by-Layer adsorption:

Zero of contact between two mica surfaces in the SFB (see below) was determined by bringing these two surfaces into adhesive contact under pure water. Then, the water was replaced by PEO in 0.1M KNO_3 salt solution and the surfaces allowed to incubate for 14 - 16 hours. PEO solutions at concentration 150 μg/mL were prepared by dissolving the polymer in 0.1M KNO_3 solution at room temperature and stirring at 40 °C for 48 hours. Following incubation the excess polymer was first washed with 0.1M KNO_3 followed by pure conductivity water, and then the normal and shear force profiles were measured between the adsorbed-polymer-bearing surfaces. Then the water was replaced by 0.5 mM liposome dispersion, allowed to incubate for 4 hrs, and normal and shear profiles were then carried out.

Surface force balance (SFB)

The procedures of the mica-SFB technique have been described in detail elsewhere.[42] To summarize briefly: the SFB technique monitors the bending of two orthogonal leaf springs, a normal spring K_N and a shear spring K_S (shown schematically in the inset to Figure 4) to measure the normal (F_n) and shear (F_s) forces applied to two curved, back-silvered, atomically-smooth mica surfaces, in a crossed-cylinder configuration (mean radius of curvature R). Motion of the surfaces relative to each other is applied via a fine screw and a differential spring, while fine motion (to ±2-3 Å), both lateral and normal to each other, is applied via a sectored piezoelectric tube. The bending of the normal-force spring K_N is determined via the surface separation D, which is optimally measured to ±2–3 Å using multiple beam interferometry by monitoring the wavelength of optical interference fringes of equal chromatic order (FECO). An air-gap capacitor is used to monitor the bending of the shear-force spring K_S which then provides a direct measure of F_s.

Normal force profiles $F_n(D)$ and shear force traces $F_s(t)$ were recorded in the same approach and separation cycles. As the surfaces were progressively compressed $F_n(D)/R$ is, in the Derjaguin approximation valid here, proportional to the interaction energy per unit area between two flat parallel surfaces obeying the same force law, and is a means of normalizing results obtained using different curvature surfaces.[43] At each surface separation, lateral motion of the upper surface was applied for one minute, both during compression and upon separation of the surfaces. Shear profiles were taken by directly measuring the response of the lower surface (manifested as bending of the shear spring K_s) to this lateral motion. The lateral motion amplitudes (applied by the sectored PZT actuator), Δx_0, ranged from 200–1200 nm while the applied shear velocities v_s ranged from 10–600 nm s^{-1}. Shear forces F_s are measured from the plateau regime of the friction-force *vs.* time traces (shown later).

In cases where a clear plateau is not discernible, the magnitude of the weak shear forces are determined either by filtering the signal about the drive frequency, or by fast Fourier transform of the data

to yield F_s at the drive frequency[12]; the two approaches yield similar values of F_s. The results presented here are based on 2-3 independent experiments (different pairs of mica sheets) for each configuration, carried out in temperature-stabilized rooms at 25 ± 0.2 °C.

The normal compressive loads cause an elastic flattening of the curved surfaces, of area A, mostly due to compression of the glue supporting the mica sheet. This is clearly observed as flattening of radius a at the tips of the interference fringes. The mean pressure, P, between the compressed surfaces can then be directly evaluated from the dimensions of this flattened area as $P = F_n/A = F_n/\pi a^2$. The flattening of contacting, non-adhering surfaces can be also evaluated from Hertzian contact mechanics,[44] and be used for pressure evaluation. This method is preferred for cases of small a which may not be readily measureable from the fringe shapes, where $a = (F_nR/K)^{1/3}$, K being the known effective elastic modulus (determined separately) of the glue/mica layers.

Atomic Force Microscopy (AFM)

Surface topography was determined by using an atomic force microscope (MFP-3D SA, Oxford Instruments Asylum Research, Inc., Santa Barbara). The surfaces were scanned in non-contact mode under conductivity water using a silicon nitride V-shaped cantilever having a nominal spring constant of 0.35 N/m with a pyramidal silicon nitride tip with a nominal radius of 2 nm (SNL, Bruker).

Cryo SEM:

The samples were rapidly frozen in liquid ethane at -160 °C using a custom-made spring plunger. Ice was sublimated at -80 °C for 1.5-2 hours. The samples were rotary-shadowed with 3-5 nm Pt/C at an angle of 45°. Thereafter, the samples were transferred using a vacuum cryo-transfer (VCT) device (model 100, Leica Microsystems, Vienna) to an Ultra 55 high resolution scanning electron

microscope (cryo SEM) (Zeiss, Germany) equipped with a cryo stage for cryo imaging of biological samples and synthetic soft materials. Samples were observed at voltages of 0.9-10 kV by means of an in-lens secondary electron detector at a temperature of -120°C.

Dynamic Light Scattering:

The size distribution of the liposomes was obtained by Viscotek model 802 dynamic light scattering (DLS) at laser wavelength of 830 nm and by Malvern's Zetasizer Nano ZSP.

Results and discussion

Unless otherwise stated, all PEO samples used were of M_w = 110 kDa.

Size-distribution of PC-SUVs and their complexes with PEO

The size of the PEO and of the PC vesicles were determined using DLS. Figure 1 shows the hydrodynamic size distribution of PEO alone, of DSPC-SUVs alone, and of the DSPC-SUVs together with the PEO, all in the 0.1M KNO_3 solution (results in water were rather similar).

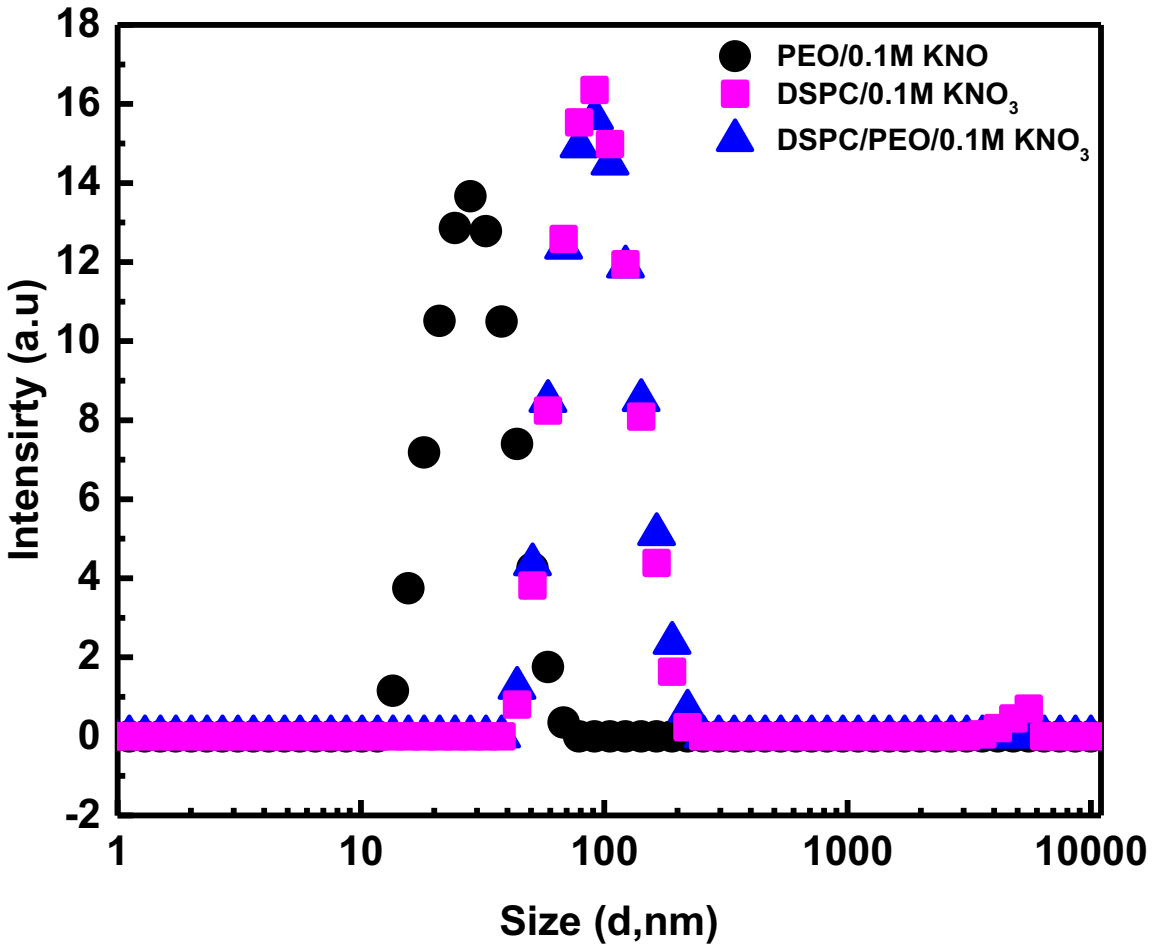

Figure 1: Size distribution of PEO, DSPC-SUVs, and their mixture, in 0.1 M KNO_3. PEO (concentration 150 µg/mL) (circles); DSPC-SUVs prepared in salt, concentration 0.5 mM (squares); and a mixture of DSPC-SUVs (concentration 0.45 mM) and PEO (concentration 15 µg/mL) (triangles)**.**

As seen in Figure 1, the hydrodynamic diameter of PEO (110K) in 0.1M KNO_3 was 28 nm. The hydrodynamic diameters of the DSPC-SUVs either alone, or together with PEO in 0.1M KNO_3, were 90±5 nm; the interesting feature here is that the PEO DLS peak at 28 nm disappeared from the polymer/liposome mixture, indicating that essentially all the PEO in the solution adsorbed to the liposomes outer surface. The fact that there is no significant increase in the liposome size as determined by DLS prior to and following the PEO adsorption suggests that the PEO adsorbs to the vesicle surfaces in layers that are much flatter than its free-floating hydrodynamic radius of *ca.* 14 nm. An estimate based on the concentrations of PEO and liposomes in the DLS solution indicates

ca. 20±2 PEO molecules are adsorbed onto each vesicle. This corresponds to a low adsorbance of *ca.* 0.1 mg/m^2 of the PEO on the vesicle surface, compared with an adsorbance 3 - 4 mg/m^2 for PEO of similar M_w adsorbed from 0.1M KNO_3 onto mica[45], which would be consistent with a thin adsorbed polymer layer (< 5 nm) on the vesicles and thus with the DLS measurements.

Imaging of Liposomes on PEO layers adsorbed on mica:

The surface structure of liposome-polymer complexes were studied by AFM and Cryo SEM. Figure 2A shows the AFM image of DSPC-SUV on PEO having a height of 10±1 nm and lateral dimension of ~ 100 nm corresponding to the adsorbed, flattened vesicles, similarly to what was previously reported by Sorkin.[9] Figure 2B shows the AFM scan of DMPC-SUVs on PEO revealing a bilayer surface with a height of 5±1 nm**.** Figure 2 (C-D) shows the AFM scan of DSPC-SUV prepared in 0.1M KNO_3 on bare mica and on PEO having a height of 10±2 nm and lateral dimension of ~ 100 nm corresponding to the adsorbed, flattened vesicles**.** We noted that AFM scans of DSPC liposomes prepared in 0.1 M KNO_3 salt solution on PEO adsorbed on mica was harder to image, probably due the presence of high concentration of salt in the system, which weakens the adsorption of liposomes on PEO/mica.

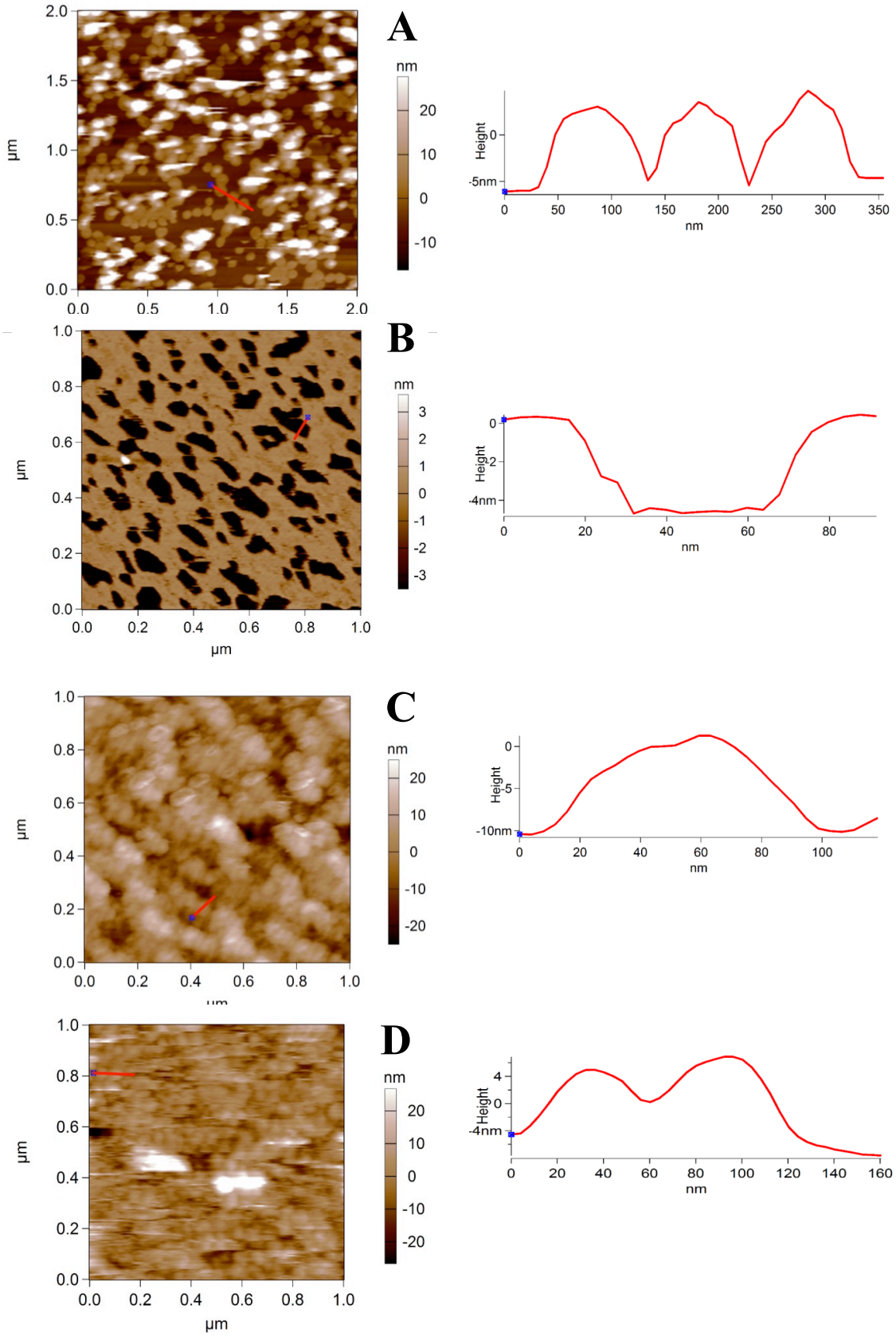

Figure 2: AFM imaging of different liposomes on mica and PEO-coated mica A) DSPC-SUVs on PEO in water, B) DMPC-SUVs on PEO in water, C) DSPC-SUVs in 0.1M KNO_3 on bare mica and D)DSPC-SUVs on PEO in 0.1M KNO_3 .

Figure 3 shows the cryo-SEM images of liposomes prepared A) in water and C) in 0.1M KNO_3 on PEO-coated mica and B) on bare mica. DMPC liposomes could not be imaged, probably due to their rupturing upon adsorption to the PEO adsorbed mica surface, compounded by damage because of the cryo-SEM preparation procedure**.**

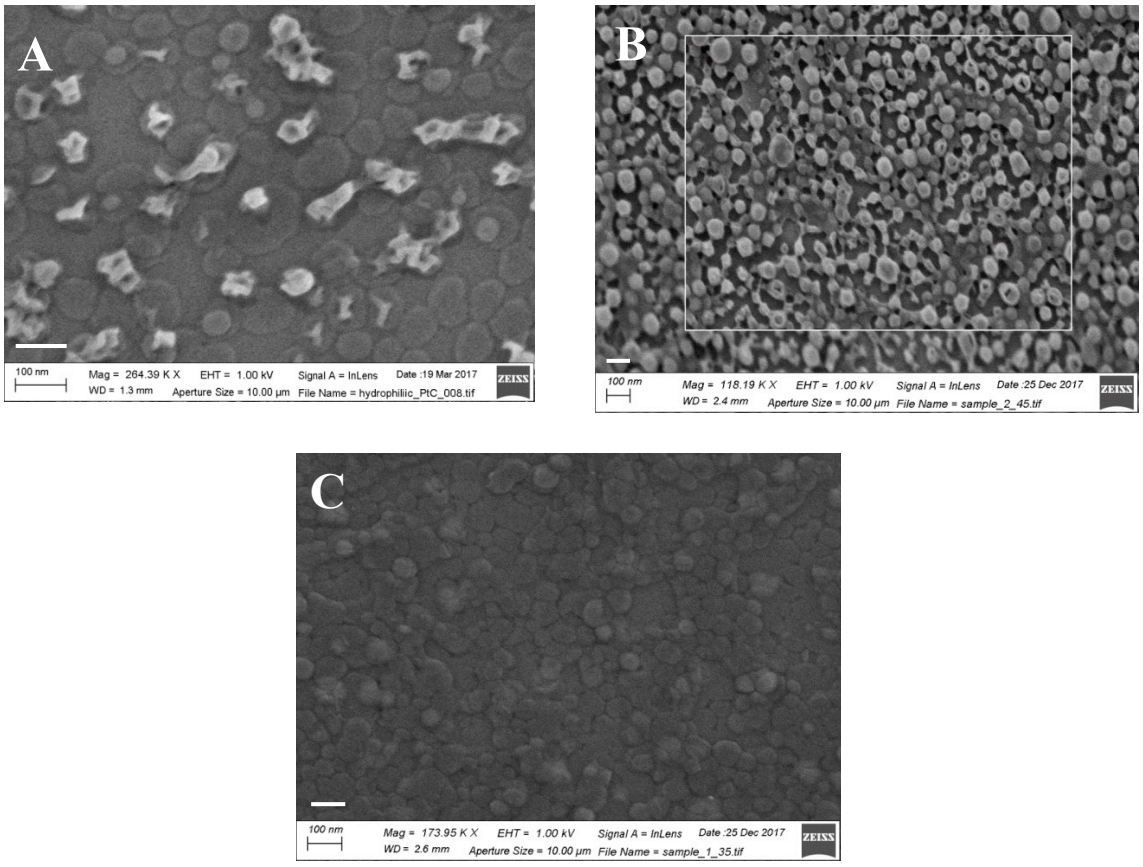

Figure 3: Cryo-SEM images of: A) DSPC-SUVs on PEO in water; B) DSPC-SUVs prepared in (0.1M KNO_3) on bare mica; and C) DSPC-SUVs prepared in (0.1M KNO_3) on PEO. Scale bars: 100 nm.

Normal and Frictional Forces between PEO/liposome complexes:

Adsorbed PEO layers:

Earlier studies show that PEO does not adsorb on mica from pure water, or from Na^+ or Li^+ salt solutions,[46] but only by co-ordination bonds via potassium ions at the mica surface (and not via van der Waals dispersion forces).[47] Normal surface interactions two mica surfaces incubated overnight in 150 μg/ml PEO solution in 0.1M KNO_3 , are presented in Figure 4. The force vs. surface separation *D* profiles, as well as the frictional behavior, agree well with previous normal force studies between PEO layers adsorbed from 0.1 KNO_3[47]. Long ranged repulsion forces commenced from *ca.* 80-100 nm, likely due to double-layer electrostatic repulsion together with steric interactions of the adsorbed polymer. On further compression, a limiting surface separation, or 'hard wall' repulsion, was measured at $D = 9 \pm 2$ nm which is again in agreement with the previous result.[47] Replacement of PEO solution by pure water resulted in no significant change in $F_n(D)$ profiles (Figure 4), showing that the PEO did not desorb despite replacing the K^+ salt solution by water. The adsorbed PEO layers, whether under bulk PEO solution or under pure water, exhibited poor lubrication properties, as shown in Figure 4 (B), with friction coefficients increasing from *ca.* 0.03 at low loads (up to $F_n \approx 20$ μN, corresponding to normal contact stresses of *ca.* 0.5 MPa) to *ca.* 0.1 at the highest loads, similar to an earlier study.[45] The friction is attributed to frictional dissipation as PEO segments rub against each other at low loads, and to bridging by the polymers at high compression, where the PEO chains making contact with the opposing mica surface.

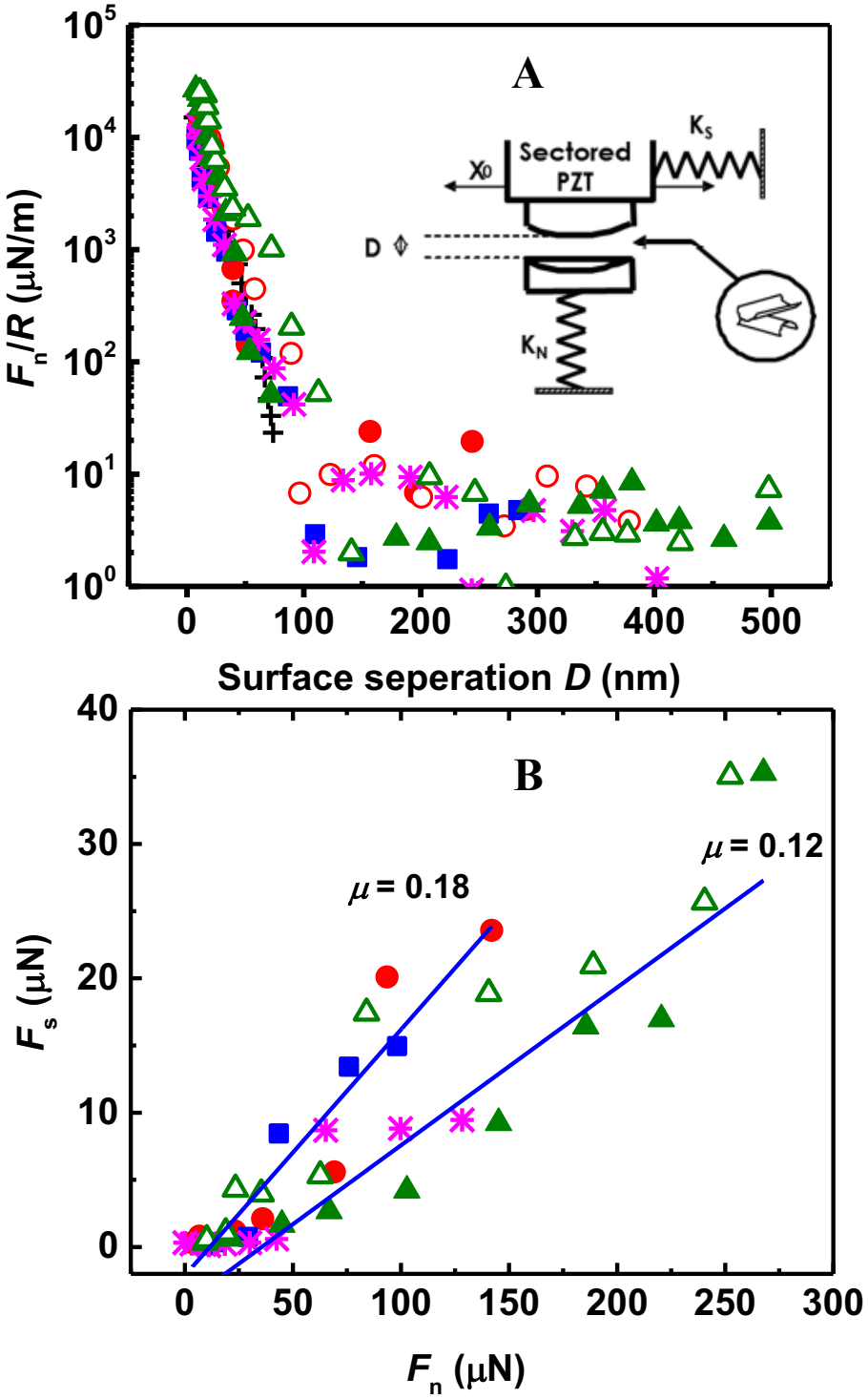

Figure 4: A) Normalized force F_n/R versus surface seperation D profiles between two mica surfaces following the incubation of 150 μg/mL PEO solution in 0.1M KNO_3 (Circle and square) and after replacement of the PEO solution by pure water (triangles and asterisks). + symbols are data from ref. 47 B) Friction force F_s versus load F_n between mica surfaces bearing PEO layers. Filled symbols are the first approach, the empty symbols are second approach, and different shapes represent different contact position or different experiments.

Liposomes on PEO coated mica surfaces (across water):

Following PEO adsorption on the mica and determination of the normal force profiles as above across water, PC- SUVs were absorbed on PEO layers by incubation in DSPC- or DMPC-SUVs dispersions at 0.5 mM lipid concentrations for 4 hours, and the resulting normal force profiles are shown in Figure 5 (A) and (B) respectively. For the case of DSPC, Figure 5(A), the force profiles between bare mica and between PEO coated mica surfaces are shown for comparison (triangles and asterisks symbols). The liposome/PEO complex surfaces exhibit a long-range repulsion, likely of steric origin due to the attached vesicle layers, commencing at D = 100 - 200 nm. With further compression, a sharp increase in repulsion is observed, with an effective hard wall (i.e. limiting thickness at high compressions) of 15 ± 2 nm in the case of DMPC-SUVs and 32 nm in the case of DSPC-SUVs attached to the adsorbed PEO layers. Comparing with the hard wall separation D = 9 ± 2 nm with PEO alone, the additional hard wall thickness corresponds to some 2 compressed liposome layers in the case of DSPC and some two compressed bilayers in the case of DMPC; that is one DSPC vesicle layer and one DMPC bilayer per PEO-coated surface respectively, which is very much in line with indications from the AFM and cryo-SEM micrographs (Figures 2, 3).

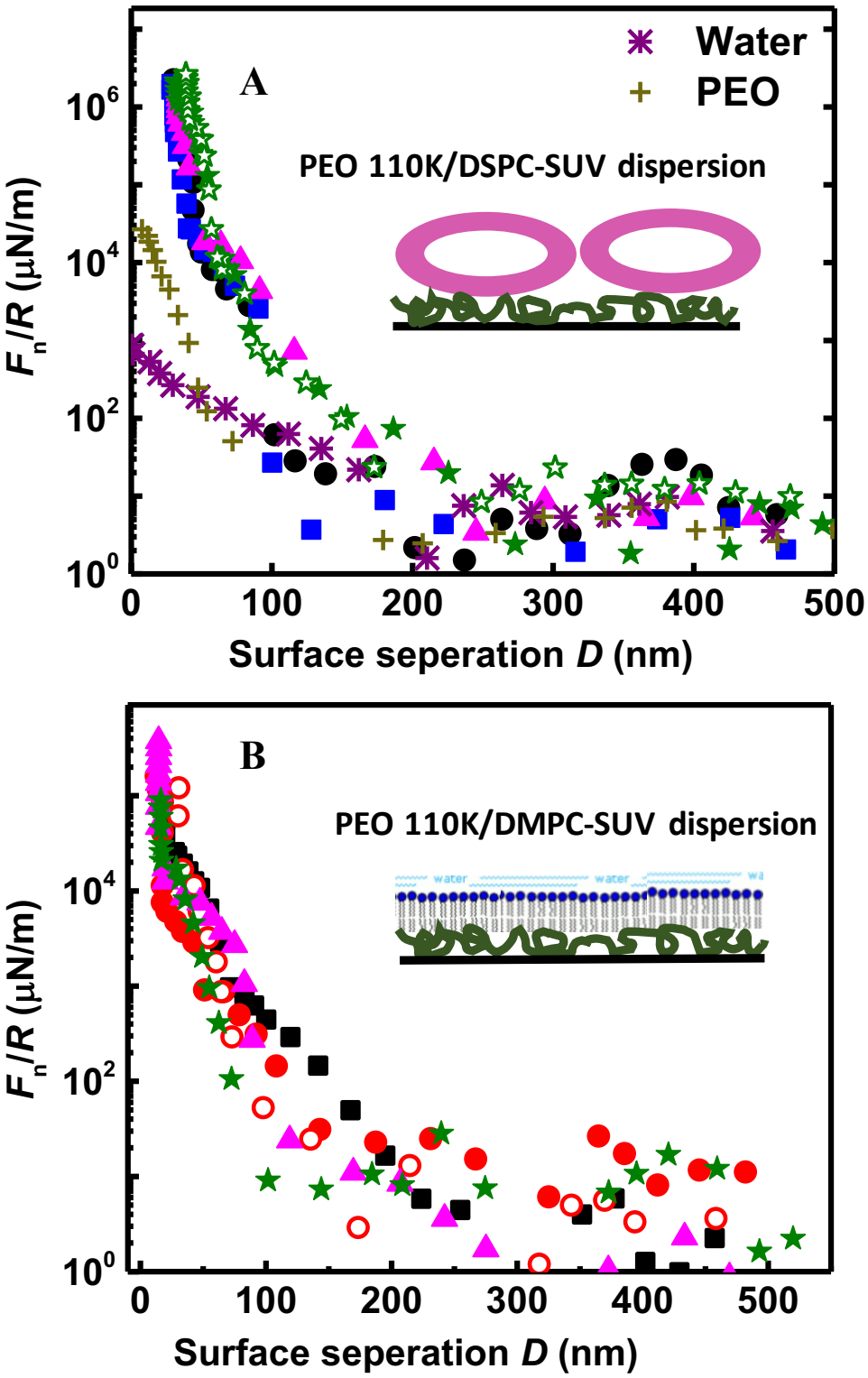

Figure 5: Force F_n/R versus surface seperation D profiles between adsorbed PEO following incubation in A.) DSPC-SUV dispersion and B.) DMPC-SUV dispersion. Filled symbols are the first approach, the empty symbols are the second approach, and different symbols represent different contact position or different experiments. In (A) are shown, for comparison, also the bare mica (asterisks) and PEO-coated mica (cross) interactions prior to adding the liposomes.

While the difference between the normal force profiles $F_n(D)/R$ for adsorbed PEO alone and following the addition of liposomes, as in Figure 5, shows the additional range of repulsion due to the lipids complexing with the adsorbed layers, the really striking differences are seen when measuring the shear or frictional forces. As seen in Figure 4(B), adsorbed PEO alone exhibits poor lubrication properties with friction coefficient of $\mu \approx 0.1$ at higher compressions; however, the complexing of lipids on the adsorbed polymer layer results in very different behavior, differing also between the two lipid types, as shown in Figures 6 and 7. Figure 6 (A-B) illustrates typical frictional traces $F_s(t)$ observed at increasing pressure for PEO-DSPC and PEO–DMPC coated mica surfaces, respectively, while Figures. 7(A-B) summarize the variation of F_s, extracted from such traces, as a function of corresponding loads F_n.

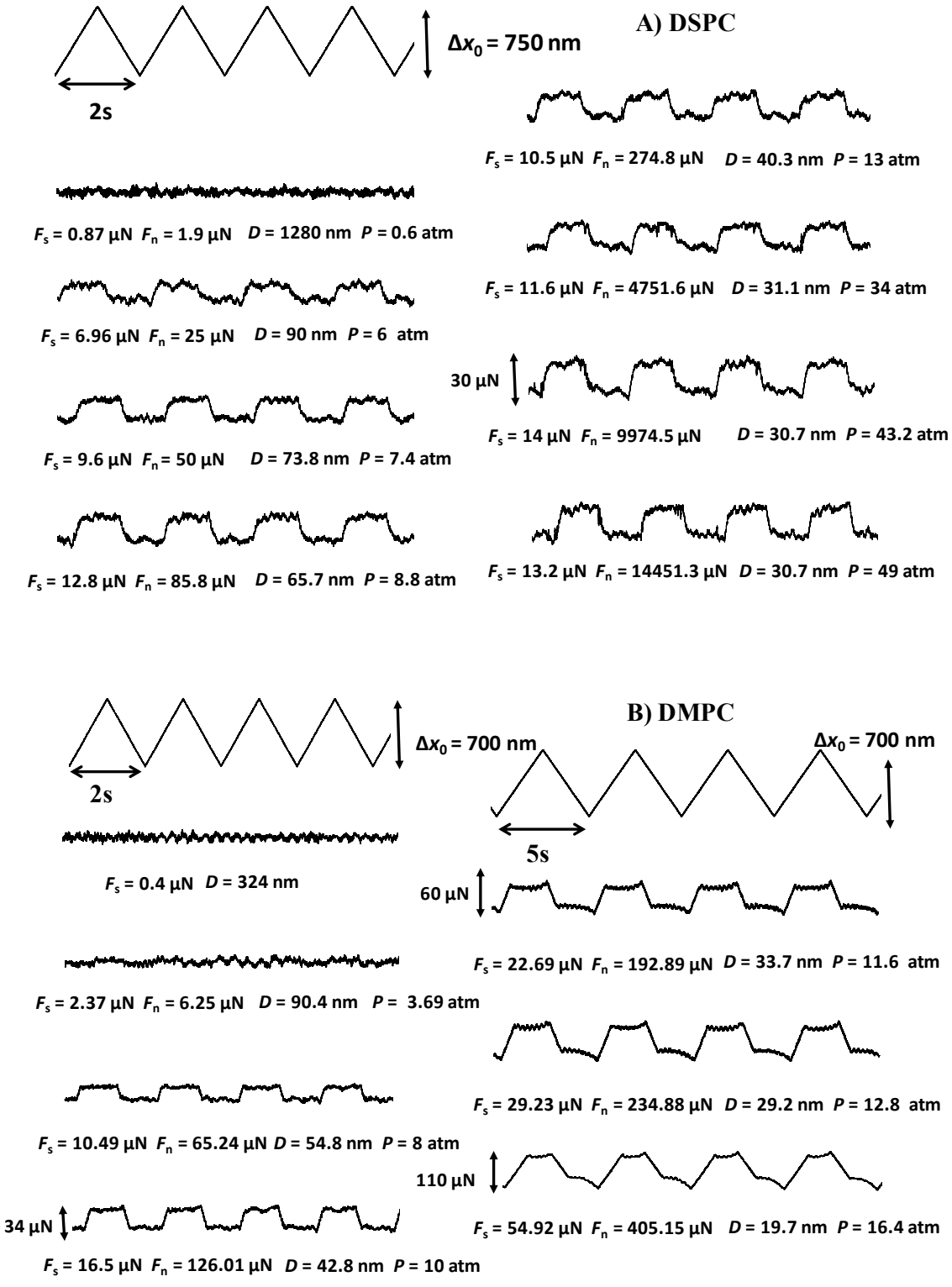

Figure 6: Typical shear traces of the frictional force $F_s(t)$ between two mica surfaces bearing different liposomes on PEO. A) PEO layers with DSPC-SUVs and B) PEO layers with DMPC-SUVs in response to a back-and-forth lateral motion.

Although the normal force profiles of DSPC and DMPC as shown in Figure 5 were broadly similar (save that their hard wall separation differed, indicating either one vesicle layer or one bilayer on the adsorbed PEO, respectively), they show very different frictional behaviour. For the DSPC layers, Figure 7(A), friction was greatly reduced with μ down to 0.0001 at the highest loads, while for DMPC, Figure 7(B), the scatter was larger, with μ largely in the range 0.06 – 0.15 (and in one measurement as low as 0.01). For the DSPC case, where the SUVs retain their integrity when attached to the PEO layers, as shown in the micrographs as well as in the normal force profiles, the low friction is attributed to boundary lubrication between the highly-hydrated phosphocholine layers exposed by each of the opposing SUV layers. We note the rapid initial rise in friction (Figure 6(A), seen also in earlier studies,[6] which is likely due to viscous losses arising from shear of the PEO/DSPC-SUV surface complexes at the lower compressions. For the DMPC case, Figure 6(B), where each surface is coated by a bilayer alone (rather than a vesicle layer), the higher frictional dissipation may be higher as a result of a less robust lipid layer (recalling that T_M = 24 °C for the DMPC is similar or slightly lower than the measurement temperature 25 °C.[9])

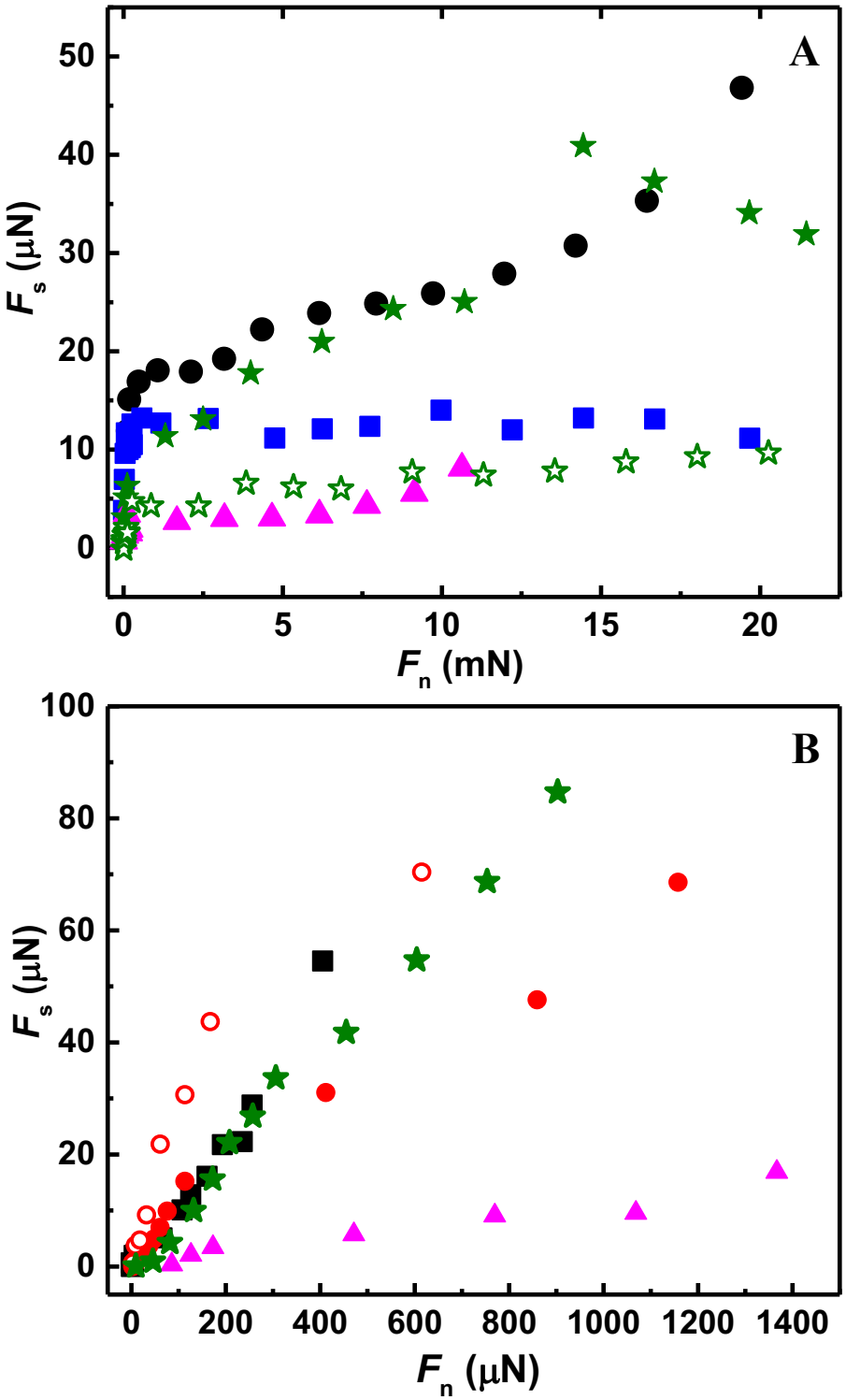

Figure 7: Friction force F_s versus normal load F_n between sliding mica surfaces of A) PEO bearing adsorbed DSPC-SUVs and B) PEO bearing adsorbed DMPC-SUVs. Filled symbols are the first approach, the empty symbols are the second approach, and different symbols represent different contact position or different experiments.

Interactions of lipid/PEO complexes across aqueous salt solutions:

Normal and shear interaction of liposomes on PEO, Figure 5 - 7, were studied across water with no added salt. However, from biological point of view, it is of interest to study such interactions closer to physiological salt concentration. Figure 8(A) shows the normal force versus surface separation *D* of DSPC-SUVs prepared under 0.1M KNO_3 on PEO-coated mica surfaces across aqueous 0.1M KNO_3 solution.

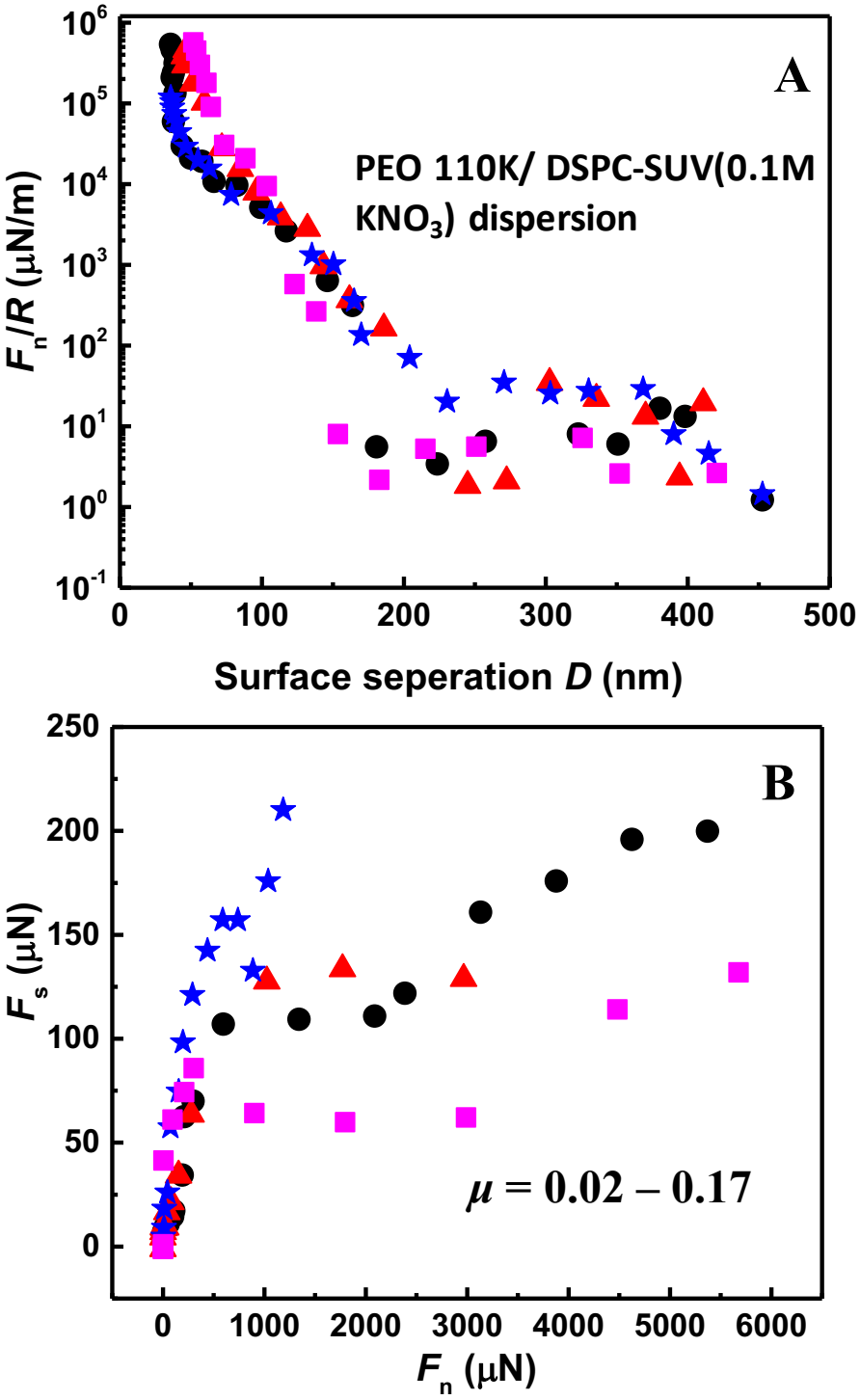

Figure 8: A) Normal force versus surface separation D of DSPC-SUV (prepared under 0.1M KNO_3) on PEO-coated mica surfaces across aqueous 0.1M KNO_3 solution. B) Shear force (F_s) as a function of normal force (F_n) for the system in (A). Different symbols represent different contact position or different experiments.

The normal force profiles $F_n(D)/R$ in Figure 8(A) exhibit a steric repulsion from $D \approx$ 200- 220 nm attributed (as for the pure water case) to steric effects due to excess liposomes weakly attached on the adsorbed PEO layer. On further compression, a sharp increase in repulsion is observed with the final ('hard wall') separation varying from 35 nm to 50 nm for different contact positions, corresponding to roughly 2 - 4 flattened DSPC-SUV layers confined between the adsorbed PEO layers (or *ca.* 1 – 2 SUV layers per surface).

Shear force measurements under 0.1M KNO_3, however, as seen in Figure 8(B) reveal a large frictional dissipation, with μ = 0.02 – 0.17 at the highest compressions, very much higher than for the DSPC/PEO surface complex under (no-added-salt) water, Figure 7(A), for which μ down to 10^{-4} was measured. This could be attributed to a number of factors. The hydration lubrication mechanism acting at the vesicle-vesicle interface at high salt concentrations may be less effective than in pure water, due to competition for the hydration water by the salt ions,[48] although measurements by Goldberg et al.[8] suggested that similar PC vesicles could provide good lubrication at high salt. It is also possible that the higher frictional dissipation arises from the adsorbed polymer itself, for example through bridging across from one mica surface to the other: in the pure water experiments such bridging would be suppressed as PEO is known not to adsorb on mica from salt-free water,[47] but it may occur in 0.1M KNO_3, from which PEO is known to adsorb on mica via K^+ bridging of PEO segments to the mica. In order to shed light on this we carried out the following experiments.

To examine the question of the effect of salt on the hydration lubrication, we adsorbed DSPC-SUVs (prepared in salt solution) on bare mica, and measured the interactions between them under different conditions. The results are shown in Figure 9, where the normal and shear interaction

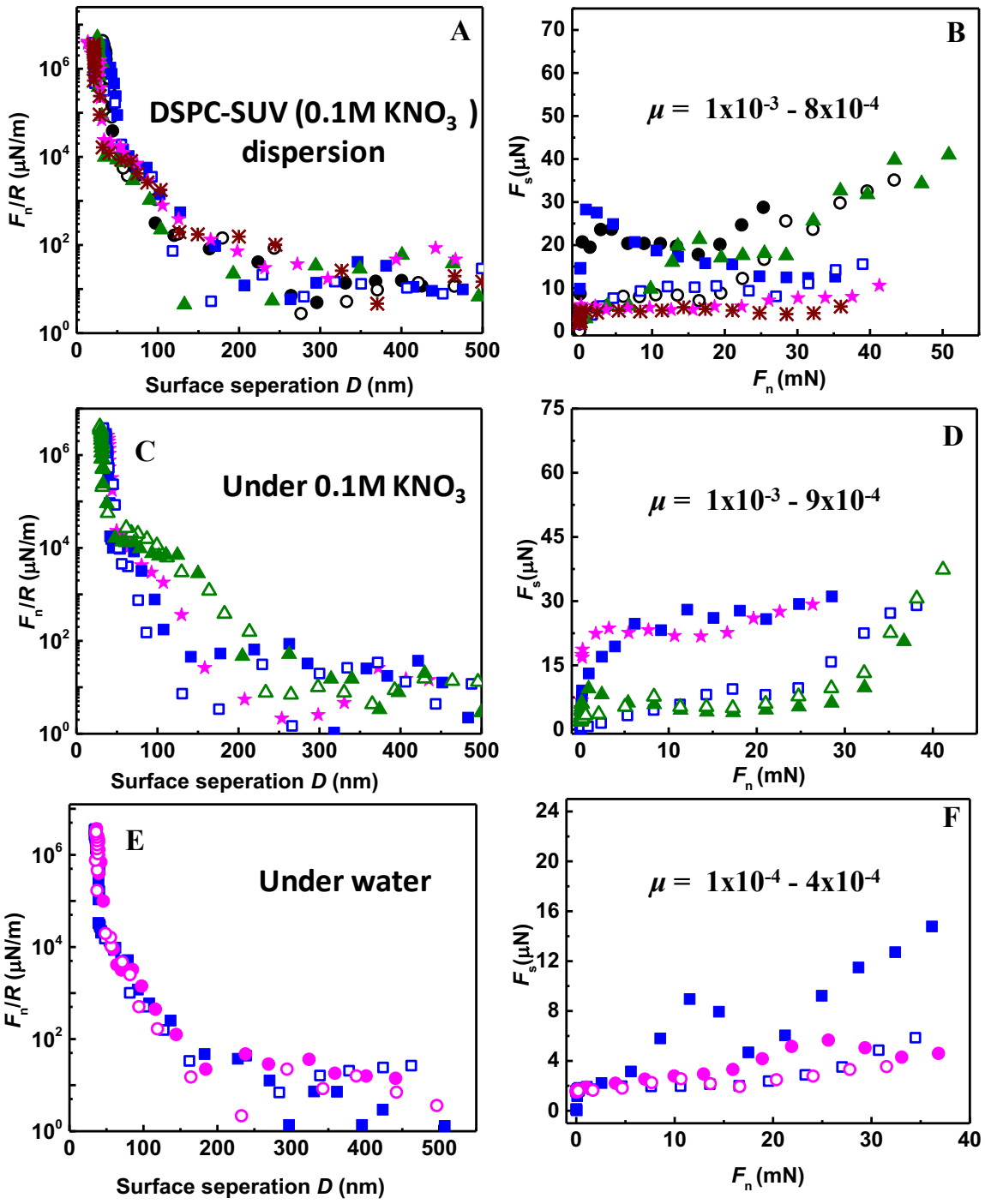

Figure 9: Normal force versus surface seperation D of DSPC-SUV prepared under 0.1M KNO_3 on bare mica surfaces across (A) Liposome solution, following 4 hours incubation (C) aqueous 0.1M KNO_3 solution and (E) pure water. Shear force (F_s) as a function of normal force (F_n) of DSPC-SUV on mica surfaces across (B) Liposome solution, (D) aqueous 0.1M KNO_3 solution and (F) pure water. Filled symbols are the first approach, the empty symbols are the second approach, and different symbols represent different contact position or different experiments.

between two bare mica surfaces are measured across: 1) DSPC-SUV dispersion prepared under 0.1M KNO_3, following 4 hours incubation in the dispersion, to allow the vesicles to coat the mica; 2) after the dispersion was replaced by 0.1M KNO_3 salt solution; 3) after the salt solution was replaced by water. We see clearly, Figures 9(A), 9(C) and 9(E), that the normal force profiles are similar for all three configurations, with 'hard wall' separations corresponding in all cases to 2-3 confined DSPC liposome layers. At the same time, the shear force profile, Figures 9(B), 9(D) and 9(F) reveal clearly that in all three cases the friction is very low, with μ values in the range 10^{-3} – $5x10^{-4}$ throughout.

The results in Figure 9, where very low friction is seen, tell us clearly that the effect of salt on hydration lubrication at the interface between the DSPC vesicles in 0.1M KNO_3 is negligible, and thus cannot be the origin of the high friction between the DSPC vesicles complexed with the PEO in 0.1M KNO_3, as in Figure 8(B).To examine therefore whether polymer bridging might be responsible for this high friction, we replaced the 110 kDa PEO with a much shorter PEO of M_w = 26 kDa, with the idea that shorter polymers have a lower likelihood of bridging, if only because their tails and loops are on average shorter. The results are shown in Figure 10. They reveal rather similar behaviour to that using the longer PEO (110 kDa), as in Figure 8, in particular that the friction coefficient, at $\mu \approx 0.02 – 0.08$, remains high relative to that in the absence of adsorbed PEO (Figure 9, where $\mu \approx 10^{-3}$ or lower) indicating that bridging may still be active, and increase the frictional dissipation on sliding, even with the shorter PEO chains.

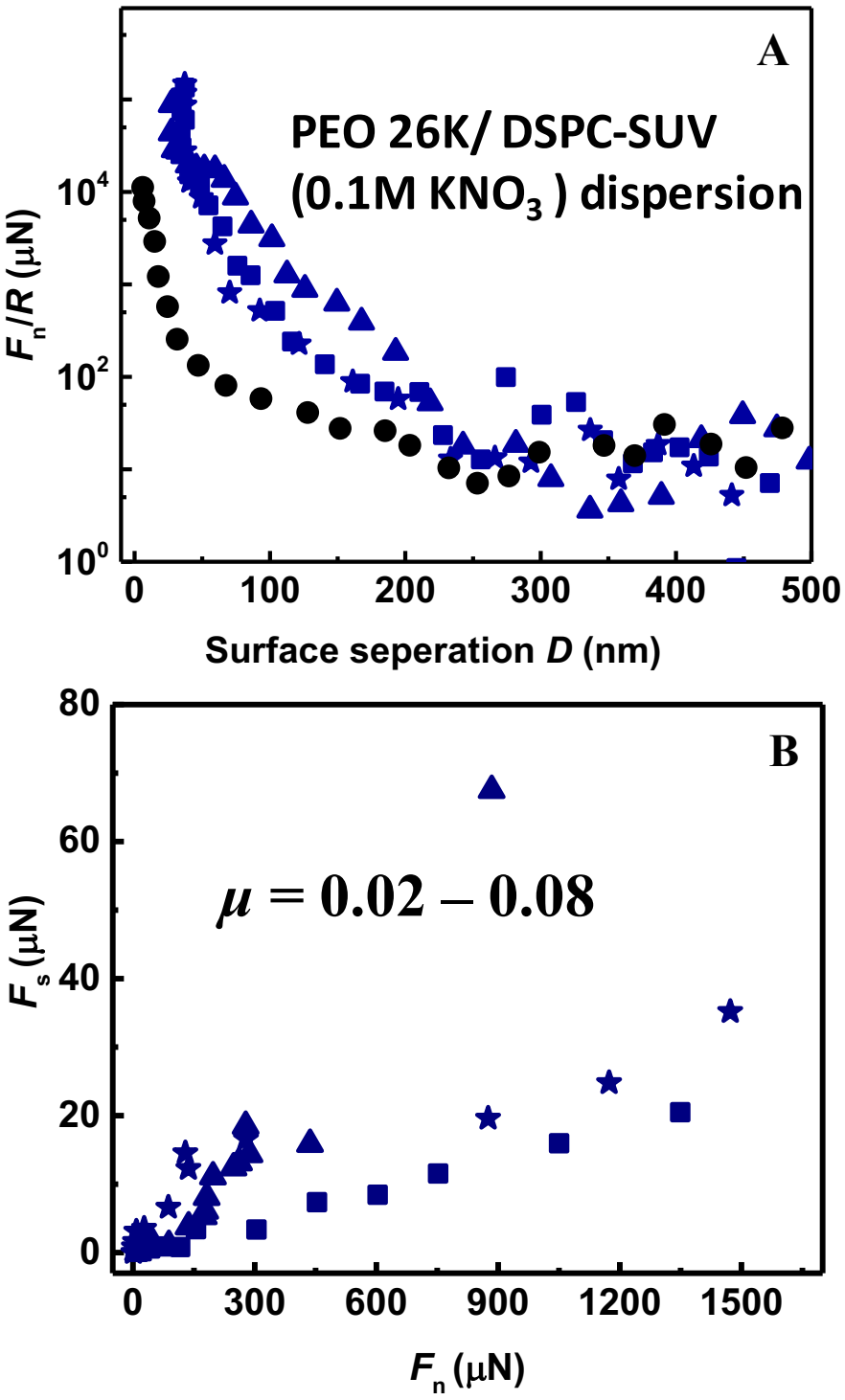

Figure 10: A) Normal force versus surface seperation D of DSPC-SUV prepared under 0.1M KNO_3 on PEO (26 K) coated mica surfaces across aqueous 0.1M KNO_3 solution. B) Shear force (F_s) as a function of normal force (F_n) of DSPC-SUV on PEO (26 K) coated mica surfaces across aqueous 0.1M KNO_3 solution. Different symbols represent different contact position or different experiments.

The experiments described above for both the adsorbed 110 kDa and 26 kDa PEO chains involved KNO_3 as the salt used to bring the aqueous medium to physiological salt concentrations, and in both cases the high friction with DSPC-SUVs is attributed to bridging. As K^+ is known to be a ligating ion for the PEO adsorption to the mica,[47] we hypothesized that changing the alkali metal ion type from potassium to sodium would prevent the bridging between the two surfaces by the PEO polymer. This is because, as shown earlier,[46] it is known that PEO does not adsorb on mica from either $LiNO_3$ or $NaNO_3$ solutions. Therefore, we adsorbed the PEO(110 kDa) on the mica surface from KNO_3 solution followed by washing the salt excess with pure water; this procedure, as seen earlier, left the adsorbed PEO layer intact on the mica surfaces. DSPC-SUVs were made in 0.1M $NaNO_3$ salt solution, and this dispersion then replaced the water in the SFB, left to incubate for 4 hours with the PEO-coated mica surfaces, and normal and shear forces were determined. Subsequently, as for the procedure shown in Figure 9, the DSPC-SUV dispersion was replaced by 0.1M $NaNO_3$, and following measurements, the salt solution was itself replaced by pure water and $F_n(D)$ and F_s were measured again. Results are shown in Figure 11, and reveal clearly that our hypothesis was correct: frictional dissipation on compression and sliding became very low again, with μ in the range *ca.* 5×10^{-4} to 8×10^{-3} in all three cases.

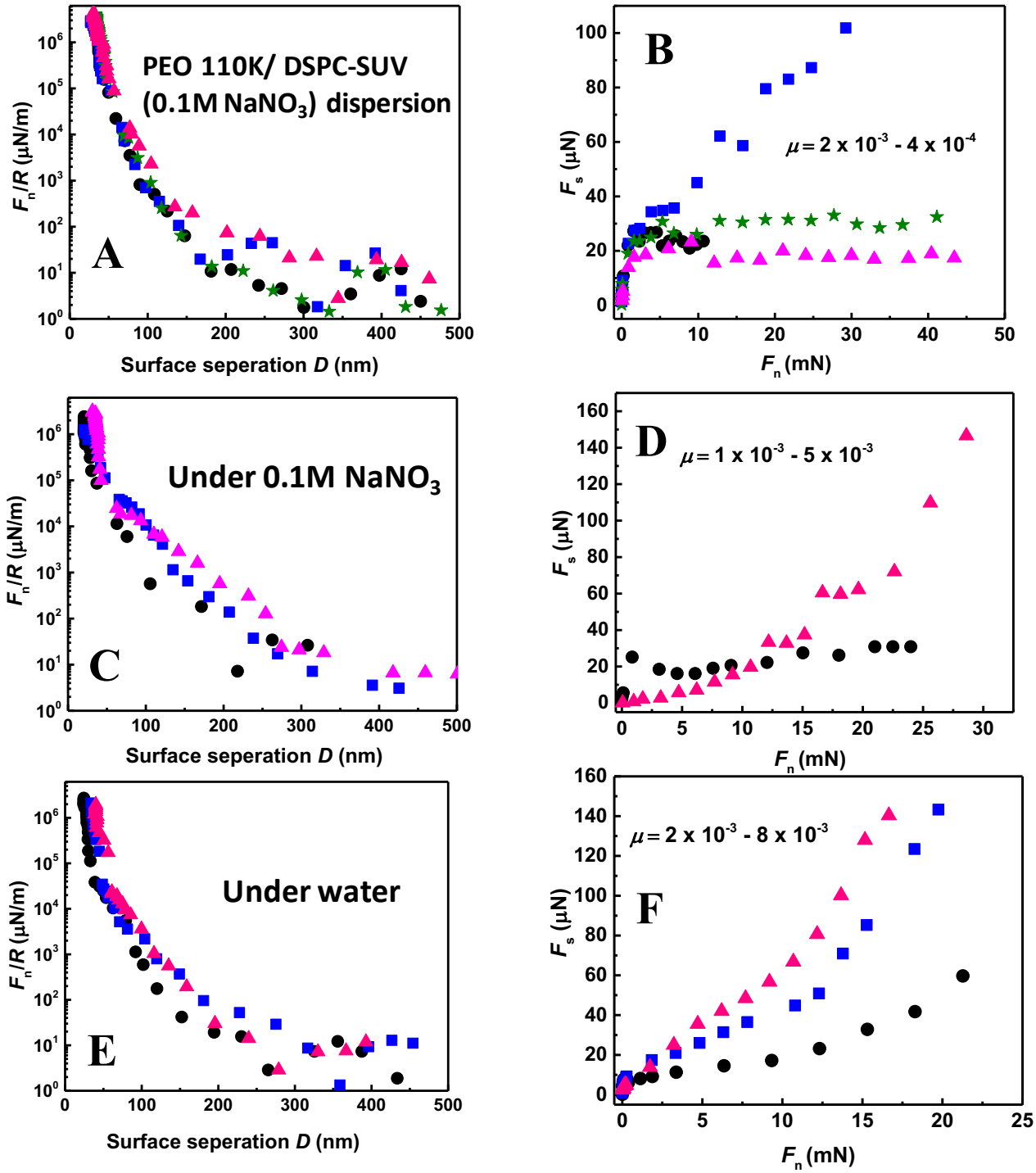

Figure 11: Normal force versus surface seperation D of DSPC-SUV prepared under 0.1M $NaNO_3$ on PEO (110K) across (A) Liposome solution, (C) aqueous 0.1M $NaNO_3$ solution and (E) pure water. Shear force (F_s) as a function of normal force (F_n) of DSPC-SUV on PEO across (B) Liposome solution, (D) aqueous 0.1M $NaNO_3$ solution and (F) pure water. Different symbols represent different contact position or different experiments.

Figure 11 shows that long ranged repulsion – likely of steric origin due to liposomes attached to the adsorbed PEO layers - was observed commencing from *ca.* 200 nm in all three cases. With further compression a final 'hard-wall' separation of *ca.* 30 nm was measured in all cases, Figure 11 (A), (C) and (E), corresponding to two compressed DSPC-SUVs vesicle layers, one on each surface (deduced from the *ca.* 9 nm thickness of the two adsorbed PEO layers, and *ca*. 20 nm thickness due to two flattened DSPC vesicles). The shear force measurements, Figure 11 (B), (D) and (F), show the low friction noted above, and confirm that little bridging occurred under the sodium salt solution, in strong contrast to the earlier measurements under KNO_3, Figure 8, where μ values were around 0.02 – 0.2. These results are summarized in Table 1.

System	**Medium**	**Friction Coefficient (μ)**	**P_{max} (atm)**	**"Hard-wall" Separation (nm)**
PEO	Water	0.07 - 0.13	9	9 ± 1
PEO (110k)/ DSPC-SUV	Water	0.002 - 0.0008	55	30 ± 2
PEO (110k)/DMPC	Water	0.02 - 0.1	31	17 ± 2
DSPC-SUV/ Mica	0.1M KNO_3	0.0001 - 0.001	70	30 ± 2
PEO (110k)/DSPC-SUV	0.1M KNO_3	0.02 - 0.17	35	35 ± 5
PEO (26k)/DSPC-SUV	0.1M KNO_3	0.01 - 0.08	22	32 ± 5
PEO (110K)/DSPC-SUV	0.1M $NaNO_3$	0.001 - 0.0008	70	30 ± 2

Table 1. Summary of sliding friction coefficient (μ), maximum pressure and "hard `wall" final separation distance for different adsorbed liposomes on PEO layer. In all cases the DSPC-SUVs were made in either water or salt solutions, corresponding to the medium in which force measurements were made.

Conclusions:

In summary, the main finding of this work concern how PC lipids, which have an important role in biological lubrication processes,[5] interact as lubricants with poly(ethylene oxide), an important polymer widely used in biological studies and in biomedical devices. We examined, in detail, how different PC-liposomes (DSPC-SUVs or DMPC-SUVs) prepared under water or under physiological-level salt concentration act as lubricating agents when complexed with adsorbed PEO. DMPC-SUVs, whose main transition temperature is lower than the room temperature of the measurements, rupture to form bilayers on PEO in water and provide poor lubrication due likely to the lower robustness of the bilayers, as discussed earlier for adsorption of these lipids on bare mica.[9] DSPC-SUVs complex as intact liposomes with the adsorbed PEO. These provide good lubrication across water, but across physiological level potassium salt (0.1M KNO_3) large frictional dissipation is seen, and attributed to bridging by the adsorbed PEO layers. When replacing the potassium salt by 0.1M $NaNO_3$, the friction coefficient again becomes very low, by some two orders of magnitude. This is attributed to suppression of PEO bridging across the sodium salt solution, in line with earlier work[46] indicating non-adsorbance of PEO on mica from sodium salt solution, and is a remarkable example where differences between the ligation properties of K^+ and Na^+ ions lead to large effects on lubrication. These insights may have practical implications wherever lubrication in physiological salt concentration is at a premium.

Acknowledgements

This research was supported by the European Research Council (Advanced Grant CartiLube), by the McCutchen Foundation and by the Israel Science Foundation (Grant 1715/2014) and was made possible in part by the historic generosity of the Harold Perlman family. We thank the PBC Fellowship Program for Outstanding Post-doctoral Fellows for financial support to S.A.Angayarkanni.

References

(1) Meins, J. F. L.; Schatz, C.; Lecommandoux, S.; Sandre, O. Hybrid polymer/lipid vesicles: state of the art and future perspectives. *Mater. Today*. **2013**, *16*, 397-402.

(2) Chiang, Y. T.; Lo, C. L. pH-Responsive polymer-liposomes for intracellular drug delivery and tumor extracellular matrix switched-on targeted cancer therapy. *Biomaterials.* **2014**, *35*, 5414-24.

(3) Sehgal, S.; Rogers, A. Polymer-coated liposomes: improved liposome stability and release of cytosine arabinoside (Ara-C) *J. Microencapsulation*. **1995**, *12*, 37-47

(4) Hills, B. A. Boundary lubrication in vivo. *Proc. Inst. Mech. Eng. H*. **2000**, *214*, 83-94.

(5) Jahn, S.; Seror, J.; Klein, J. Lubrication of Articular Cartilage. *Annu. Rev. Biomed. Eng.* **2016**, *18*, 235-58.

(6) Seror, J.; Zhu, L. Y.; Goldberg, R.; Day, A. J.; Klein, J. Supramolecular synergy in the boundary lubrication of synovial joints. *Nat Commun*. **2015**, *6*, 1-7.

(7) Duan, Y.; Liu, Y.; Zhang, C.; Chen, Z.; Wen, S. Insight into the Tribological Behavior of Liposomes in Artificial Joints. *Langmuir*. **2016**, *32*, 10957−66.

(8) Goldberg, R.; Schroeder, A.; Barenholz, Y.; Klein, J. Interactions between Adsorbed Hydrogenated Soy Phosphatidylcholine (HSPC) Vesicles at Physiologically High Pressures and Salt Concentrations. *Biophys. J.* **2011**, *100*, 2403–11.

(9) Sorkin, R.; Kampf, N.; Dror, Y.; Shimoni, E.; Klein, J. Origins of extreme boundary lubrication by phosphatidylcholine liposomes. *Biomaterials*. **2013**, *34*, 5465-75.

(10) Raja, A.; Wanga, M.; Zanderb, T.; Wieland, D. C. F.; Liu, X.; An, J.; Garamus, V. M.; Willumeit-Römer, R.; Fielden, M.; Claesson, P. M.; Dedinaite, A. D. Lubrication synergy: Mixture of hyaluronan and dipalmitoylphosphatidylcholine (DPPC) vesicles. *J. Colloid Interface Sci.* **2017**, *488*, 225-33.

(11) Sivan, S.; Schroeder, A.; Verberne, G.; Merkher, Y.; Diminsky, D.; Priev, A.; Maroudas, A.; Halperin, G.; Nitzan, D.; Etsion, I.; Barenholz, Y. Liposomes Act as Effective Biolubricants for Friction Reduction in Human Synovial Joints. *Langmuir*. **2010**, *26*, 1107-16.

(12) Raviv, U.; Klein, J. Fluidity of bound hydration layers. *Science*. **2002**, *297*, 1540-3.

(13) Klein, J. Hydration lubrication. *Friction*. **2013**, *1*, 1-23.

(14) Kipnis, A. G.; Klein, J. Normal and Frictional Interactions between Liposome-Bearing Biomacromolecular Bilayers. *Biomacromolecules*. **2016**, *17*, 2591−602.

(15) C. Allen; N. Dos Santos; R. Gallagher; G. N. C. Chiu; Y. Shu; W. M. Li; S. A. Johnstone; A. S. Janoff; L. D. Mayer; M. S. Webb; Bally, M. B. Controlling the Physical Behavior and Biological Performance of Liposome Formulations through Use of Surface Grafted Poly(ethylene Glycol). *Biosci. Rep.* **2002**, *22*, 225-49.

(16) Meier, M. A. R.; Aerts, S. N. H.; Staal, B. B. P.; Rasa, M.; Schubert, U. S. PEO-b-PCL Block Copolymers: Synthesis, Detailed Characterization, and Selected Micellar Drug Encapsulation Behavior. *Macromol. Rapid Commun.* **2005**, *26*, 1918-24

(17) Kojima, C.; Kono, K.; Maruyama, K.; Takagishi, T. Synthesis of Polyamidoamine Dendrimers Having Poly(ethylene glycol) Grafts and Their Ability To Encapsulate Anticancer Drugs. *Bioconjugate Chem.* **2000**, *11*, 910-7.

(18) Bae, K. H.; Lee, Y.; Park, T. G. Oil-Encapsulating PEO-PPO-PEO/PEG Shell Cross-Linked Nanocapsules for Target-Specific Delivery of Paclitaxel. *Biomacromolecules*. **2007**, *8*, 650-6.

(19) Hutson, C. B.; Nichol, J. W.; Aubin, H.; Bae, H.; Yamanlar, S.; Al-Haque, S.; Koshy, S. T.; Khademhosseini, A. Synthesis and Characterization of Tunable Poly(Ethylene Glycol): Gelatin Methacrylate Composite Hydrogels. *Tissue Eng Part A*. **2011**, *17*, 1713-23.

(20) Gefen, T.; Vaya, J.; Khatib, S.; Harkevich, N.; Artoul, F.; Heller, E. D.; Pitcovski, J.; Aizenshtein, E. The impact of PEGylation on protein immunogenicity. *Int. Immunopharmacol.* **2013**, *15*, 254-9.

(21) Dozier, J. K.; Distefano, M. D. Site-Specific PEGylation of Therapeutic Proteins. *Int. J. Mol. Sci.* **2015**, *16*, 25831-64.

(22) Jevsevar, S.; Kunstelj, M.; Porekar, V. G. PEGylation of therapeutic proteins. ***B**iotechnol. J.* . **2010**, *5*, 113-28.

(23) Nucci, M. L.; Shorr, R.; Abuchowski, A. The therapeutic value of poly(ethylene glycol)-modified proteins. *Adv. Drug Deliv. Rev.* **1991**, *6*, 133-51

(24) Pisal, D. S.; Kosloski, M. P.; Balu-Iyer, S. V. Delivery Of Therapeutic Proteins. *J Pharm Sci. Jun;():*. **2010**, *99*, 2557-75.

(25) Lowe, S.; Brien-Simpson, N. M. O.; Connal, L. A. Antibiofouling polymer interfaces: poly(ethylene glycol) and other promising candidates. *Polym.Chem.* **2015**, *6*, 198-212.

(26) Kim, S.; Gim, T.; Kang, S. M. Versatile, Tannic Acid-Mediated Surface PEGylation for Marine Antifouling Applications. *ACS Appl. Mater. Interfaces*. **2015**, *7*, 6412-6.

(27) Xu, L. Q.; Pranantyo, D.; Neoh, K.-G.; Kang, E.-T.; Teo, S. L.-M.; Fu, G. D. Polym. Chem. *Synthesis of catechol and zwitterion- bifunctionalized poly(ethylene glycol) for the construction of antifouling surfaces*. **2016**, *7*, 493-501.

(28) Ma, W.; Rajabzadeh, S.; Shaikh, A. R.; Kakihana, Y.; Sun, Y.; Matsuyama, H. Effect of type of poly(ethylene glycol) (PEG) based amphiphilic copolymer on antifouling properties of copolymer/poly(vinylidene fluoride) (PVDF) blend membranes. *J Memb Sci.* **2016**, *514*, 429-39.

(29) Wang, Y.; Betts, D. E.; Finlay, J. A.; Brewer, L.; Callow, M. E.; Callow, J. A.; Wendt, D. E.; DeSimone, J. M. Photocurable Amphiphilic Perfluoropolyether/Poly(ethylene glycol) Networks for Fouling-Release Coatings. *Macromolecules*. **2011**, *44*, 878-85.

(30) Yuan, S.; Wan, D.; Liang, B.; Pehkonen, S. O.; Ting, Y. P.; Neoh, K. G.; Kang, E. T. Lysozyme-Coupled Poly(poly(ethylene glycol) methacrylate) - Stainless Steel Hybrids and Their Antifouling and Antibacterial Surfaces. *Langmuir*. **2011**, *27*, 2761-74.

(31) Liu, S. Q.; Yang, C.; Huang, Y.; Ding, X.; Li, Y.; Fan, W. M.; Hedrick, J. L.; Yang, Y.-Y. Antimicrobial and Antifouling Hydrogels Formed In Situ from Polycarbonate and Poly(ethylene glycol) via Michael Addition *Adv. Mater.* **2012**, *24*, 6484-9.

(32) Zhu, J. Bioactive modification of poly(ethylene glycol) hydrogels for tissue engineering. *Biomaterials*. **2010**, *31*, 4639-56.

(33) Ovsianikov, A.; Malinauskas, M.; Schlie, S.; Chichkov, B.; Gittard, S.; Narayan, R.; Löbler, M.; Sternberg, K.; Schmitz, K.-P.; Haverich, A. Three-dimensional laser micro- and nano-structuring of acrylated poly(ethylene glycol) materials and evaluation of their cytoxicity for tissue engineering applications. *Acta Biomater.* **2011**, *7*, 967-74.

(34) DeKosky, B. J.; Dormer, N. H.; Ingavle, G. C.; Roatch, C. H.; Lomakin, J.; Detamore, M. S.; Gehrke, S. H. Hierarchically Designed Agarose and Poly(Ethylene Glycol) Interpenetrating Network Hydrogels for Cartilage Tissue Engineering. *Tissue Eng Part C*. **2010**, *16*, 1-10.

(35) Park, Y.; Lutolf, M. P.; Hubbell, J. A.; Hunziker, E. B.; Wong, M. Bovine Primary Chondrocyte Culture in Synthetic Matrix Metalloproteinase-Sensitive Poly(ethylene glycol)-Based Hydrogels as a Scaffold for Cartilage Repair. *Tissue Eng Pt A*. **2004**, *10*, 515-22.

(36) Bryant, S. J.; Anseth, K. S. Hydrogel properties influence ECM production by chondrocytes photoencapsulated in poly(ethylene glycol) hydrogels. *J Biomed Mater Res.* **2002**, *59*, 63-72.

(37) Cui, X.; Breitenkamp, K.; Finn, M. G.; Lotz, M.; D'Lima, D. D. Direct Human Cartilage Repair Using Three-Dimensional Bioprinting Technology. *Tissue Eng Part A*. **2012**, *18, Numbers ,* , 1304-12.

(38) Hwang, Y.; Sangaj, N.; Varghese, S. Interconnected Macroporous Poly(Ethylene Glycol) Cryogels as a Cell Scaffold for Cartilage Tissue Engineering. *Tissue Eng Part A*. **2010**, *16*, 3033-41.
(39) Musumeci, G.; Loreto, C.; Carnazza, M. L.; Coppolino, F.; Cardile, V.; Leonardi, R. Lubricin is expressed in chondrocytes derived from osteoarthritic cartilage encapsulated in poly(ethylen e glycol) diacrylate scaffold *Eur. J. Histochem.* **2011**, *55*, 162-8.
(40) Iwanaga, K.; Ono, S.; Arioka, K.; Kakemi, M.; Morimoto, K.; Yamashita, S.; Namba, Y.; Oko, A. Application of Surface-Coated Liposomes for Oral Delivery of Peptide: Effects of Coating the Liposome's Surface on the GI Transit of Insulin. *J. Pharm. Sci.* **1999**, *88*, 248-52.
(41) Minato, S.; Iwanaga, K.; Kakemi, M.; Yamashita, S.; Oku, N. Application of polyethyleneglycol (PEG)-modified liposomes for oral vaccine: effect of lipid dose on systemic and mucosal immunity. *Journal of Controlled Release*. **2003**, *89*, 189-97.
(42) Kumacheva, E.; Klein, J. Simple liquids confined to molecularly thin layers. II. Shear and frictional behavior of solidified films. *J. Chem. Phys.* **1998**, *108*, 7010-22.
(43) Israelachvili, J. N. *Intermolecular and Surface Forces, 3rd Edition*; Academic Press: Burlington: MA, 2011.
(44) Johnson, K. L. *Contact mechanics*; Cambridge university, 1987.
(45) Chai, L.; Klein, J. Shear Behavior of Adsorbed Poly(ethylene Oxide) Layers in Aqueous Media. *Macromolecules*. **2008**, *41*, 1831-8.
(46) Chai, L.; Goldberg, R.; Kampf, N.; Klein, J. Selective Adsorption of Poly(ethylene oxide) onto a Charged Surface Mediated by Alkali Metal Ions. *Langmuir*. **2008**, *24*, 1570-6.
(47) Chai, L.; Klein, J. Role of Ion Ligands in the Attachment of Poly(ethylene oxide) to a Charged Surface. *J. Am. Chem. Soc*. **2005**, *127*, 1104-5.
(48) Chen, M.; Briscoe, W. H.; Armes, S. P.; Klein, J. Lubrication at Physiological Pressures by Polyzwitterionic Brushes. *Science*. **2009**, *323*, 1698-701.